ISSN 1674-1056
http://cpb.iphy.ac.cn
http://iopscience.iop.org/cpb
中国物理 B
Chinese Physics
中国物理
Chinese Physics B

Pressure-induced structural evolution of apatite-type $La_{9.33}Si_6O_{26}$

Guangchao Yin(尹广超), Hong Yin(殷红), Meiling Sun(孙美玲), Wei Gao(高伟)
Citation: Chin. Phys. B . 2018, 27(1): 018202. **doi:** 10.1088/1674-1056/27/1/018202

Journal homepage: http://cpb.iphy.ac.cn; http://iopscience.iop.org/cpb

What follows is a list of articles you may be interested in

Structural and size evolution of indium nanoparticles embedded in aluminum synthesized by ion implantation

Yan-Xia Yan(晏艳霞), Meng Liu(刘孟), Mei-Juan Hu(胡梅娟), Hong-Zhi Zhu(朱宏志), Huan Wang(王欢)
Chin. Phys. B . 2017, 26(12): 126101. **doi:** 10.1088/1674-1056/26/12/126101

High pressure x-ray diffraction techniques with synchrotron radiation

Jing Liu(刘景)
Chin. Phys. B . 2016, 25(7): 076106. **doi:** 10.1088/1674-1056/25/7/076106

Interfacial transport in lithium-ion conductors

Shaofei Wang(王少飞) and Liquan Chen(陈立泉)
Chin. Phys. B . 2016, 25(1): 018202. **doi:** 10.1088/1674-1056/25/1/018202

Closed-form solution of mid-potential between two parallel charged plates with more extensive application

Shang Xiang-Yu, Yang Chen, Zhou Guo-Qing
Chin. Phys. B . 2015, 24(10): 108203. **doi:** 10.1088/1674-1056/24/10/108203

Aggregation of fullerene (C_{60}) nanoparticle：A molecular-dynamic study

He Su-Zhen, Merlitz Holger, Wu Chen-Xu
Chin. Phys. B . 2014, 23(4): 048201. **doi:** 10.1088/1674-1056/23/4/048201

Pressure-induced structural evolution of apatite-type $La_{9.33}Si_6O_{26}$*

Guangchao Yin(尹广超)[1], Hong Yin(殷红)[2], Meiling Sun(孙美玲)[1], and Wei Gao(高伟)[2,†]

[1] *Functional Molecular Materials Laboratory, School of Physics and Optoelectronic Engineering, Shandong University of Technology, Zibo* 255000, *China*
[2] *State Key Laboratory of Superhard Materials, Jilin University, Changchun* 130012, *China*

(Received 28 July 2017; revised manuscript received 6 September 2017; published online 28 November 2017)

The pressure-induced structural evolution of apatite-type $La_{9.33}Si_6O_{26}$ was systematically studied using *in situ* synchrotron x-ray diffraction (XRD). The XRD spectra indicated that a subtly reversible phase transition from $P6_3/m$ to $P6_3$ symmetry occurred at $\sim$ 13.6 GPa because of the tilting of the SiO_4 tetrahedra under compression. Furthermore, the $La_{9.33}Si_6O_{26}$ exhibited a higher axial compression ratio for the *a*-axis than the *c*-axis, owing to the different axial arrangement of the SiO_4 tetrahedra. Interestingly, the high-pressure phase showed compressibility unusually higher than that of the initial phase, suggesting that the low $P6_3$ symmetry provided more degrees of freedom. Moreover, the $La_{9.33}Si_6O_{26}$ exhibited a lower phase transition pressure (P_T) and a higher lattice compression than $La_{10}Si_6O_{27}$. Comparisons between $La_{9.33}Si_6O_{26}$ and $La_{10}Si_6O_{27}$ provided a deeper understanding of the effect of interstitial oxygen atoms on the structural evolution of apatite-type lanthanum silicates (ATLSs).

Keywords: lanthanum silicates, structural evolution, interstitial oxygen atoms, compressibility

PACS: 82.45.Gj, 61.05.cp, 81.40.Vw **DOI:** 10.1088/1674-1056/27/1/018202

1. Introduction

Apatite-type lanthanum silicates (ATLSs) with the general formula $La_{9.33+x}(SiO_4)_6O_{2+1.5x}$ ($0 \le x \le 0.67$) have been gaining widespread attention owing to their potential applications in gas-sensing and fuel cell devices.[1–16] ATLSs have an especially hexagonal apatite structure (Fig. 1), which is beneficial for conducting oxygen ions.[17–19] In this hexagonal structure, isolated SiO_4 tetrahedra are piled up along the *c*-axis to form unique oxide ion channels, and there are four oxygen sites (O1, O2, O3, and O4) in the structure when the La composition is stoichiometric (i.e., $x = 0$). When $0 < x \le 0.67$, a fifth oxygen site (i.e., interstitial oxygen, O5) emerges and is located close to the SiO_4 tetrahedra, which can also play a crucial role in conducting oxygen ions and improving the structural properties.[10,16] Prior research studies have indicated that the apatite-type structure is very flexible and sensitive to external forces.[20–27] However, most investigations to date have focused on the electrical properties of ATLSs; hence, the lack of systematic studies on the structural evolution of ATLSs under applied external forces.

Recently, we used *in situ* synchrotron x-ray diffraction (XRD) to investigate ATLS under high pressure to investigate the structural evolution and corresponding structural formation/alteration mechanism of ATLS under external forces.[28,29] We found that the flexibility of the apatite structure was mainly dominated by the isolated SiO_4 tetrahedra and that the compressibility was mainly dominated by the La–O polyhedral environment.[29] Moreover, we found that for the ATLS, similar to what happens in scheelite-type ABO_4 compounds, doping the Si sites with a larger cation (e.g., Mg^{2+}) increased the r_{SiO_4}/r_{La} ratio, thus enhancing the P_T and lowering the axial compressibility of the ATLS.[28] However, previous studies mainly focused on ATLS with interstitial oxygen atoms, so the detailed structural alteration mechanism of ATLS has not been rigorously determined because of the lack of comparative data to illuminate the effect of interstitial oxygen atoms on the structural evolution of ATLS under compression. Therefore, it is crucial to study in detail the behaviors of stoichiometric oxygen-interstitial-free ATLS ($La_{9.33}Si_6O_{26}$) under high pressure to gain insight into the structural properties of ATLS.

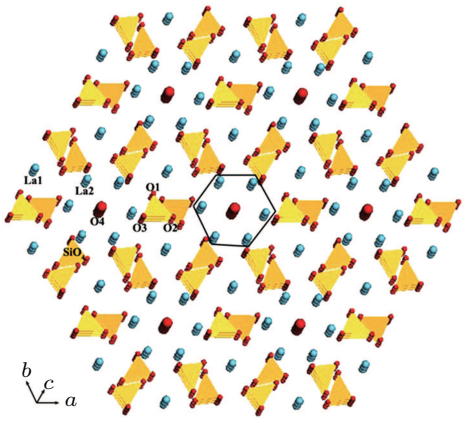


Fig. 1. (color online) Illustration of the "microporous" structure of ATLS.

*Project supported by the Natural Science Foundation of Shandong Province, China (Grant Nos. ZR2015AQ010 and ZR2016FB16) and the Open Project Fund of State Key Laboratory of Superhard Materials of China (Grant No. 201509).

†Corresponding author. E-mail: gwei@jlu.edu.cn

© 2018 Chinese Physical Society and IOP Publishing Ltd

In the present study, the pressure-induced structural evolution of apatite-type $La_{9.33}Si_6O_{26}$ was systematically investigated using *in situ* synchrotron XRD. A subtly reversible phase transition was observed at $\sim$ 13.6 GPa. The pressure dependence of the cell parameters a, c, V, and the bulk modulus were systematically analyzed. Moreover, the behavior of $La_{9.33}Si_6O_{26}$ under a high pressure was compared with those of $La_{10}Si_6O_{27}$.

2. Experimental

Apatite-type $La_{9.33}Si_6O_{26}$ powders were synthesized by the simple NaCl molten-salt method outlined in Ref. [10]. Figure 2 shows that the $La_{9.33}Si_6O_{26}$ powders used here showed a pure apatite-type structure (Fig. 2(a)), consisting of homogeneous 100–200-nm-diameter single crystals (Figs. 2(b)–2(d)). The high-pressure synchrotron XRD experiments were performed at the high-pressure station of the Beijing Synchrotron Radiation Facility (BSRF) with a synchrotron x-ray source of $\lambda = 0.6199$ Å. A symmetric diamond anvil cell (DAC) with 400-μm-culet diamond anvils was utilized to generate high pressure. A 120-μm-diameter hole was drilled in the center of T-301 stainless steel to prepare the sample chamber. Small ruby balls were inserted into the sample for *in situ* pressure calibration, and silicone grease was used as the pressure medium. The high-pressure data were collected and analyzed by a MAR165 CCD detector and FIT2D software, respectively.[30]

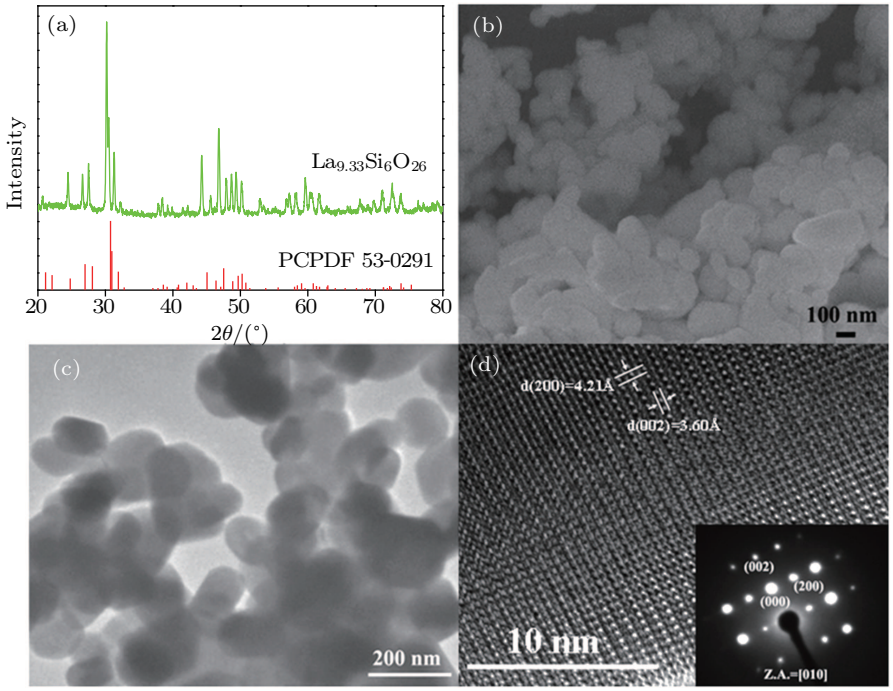


Fig. 2. (color online) (a) XRD, (b) SEM, (c) TEM, (d) HRTEM, and SAED (the inset of panel (d)) patterns of the $La_{9.33}Si_6O_{26}$ powders.

3. Results and discussion

Representative high-pressure XRD patterns for the $La_{9.33}Si_6O_{26}$ are displayed in Fig. 3. All the diffraction peaks typically weaken and shift toward higher angles with increasing pressure.[31–33] When the $La_{9.33}Si_6O_{26}$ is compressed to $\sim$ 13.6 GPa, two new diffraction peaks emerge, indicating a phase transition occurs. When the pressure is increased to $\sim$ 15.9 GPa, the new peaks completely replace the original ones, implying that the phase transition is complete. Notably, the phase transition is reversible; that is, the initial phase is recovered upon decompression. Compared with $La_{10}Si_6O_{27}$ ($P_T = 14.5$ GPa),[29] the $La_{9.33}Si_6O_{26}$ exhibits a slightly lower P_T, which could be related to the absence of interstitial oxygen atoms in the $La_{9.33}Si_6O_{26}$. According to previous studies,[28,34] P_T increases with increasing r_{SiO_x}/r_{La} ratio, where r_{SiO_x} and r_{La} represent the radii of polyhedral SiO_x units and La cations, respectively. The $La_{10}Si_6O_{27}$ contains the interstitial oxygen (O5) sites close to the SiO_4 tetrahedra, facilitating the formation of hexahedral SiO_5 units distinctly larger than the tetrahedral SiO_4 units.[35,36] As a result, the $La_{9.33}Si_6O_{26}$ exhibits a slightly lower P_T than the $La_{10}Si_6O_{27}$, indicating that the interstitial oxygen atoms could increase the P_T of the ATLS.

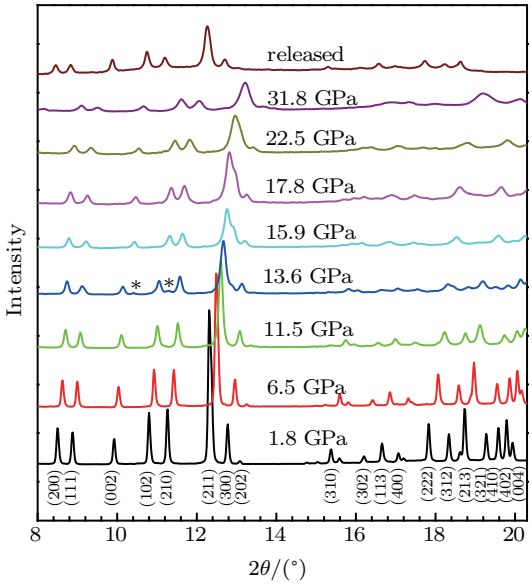


Fig. 3. (color online) Representative high-pressure XRD patterns of $La_{9.33}Si_6O_{26}$ at various pressures.

To confirm the phase transformation mechanism, both the initial and high-pressure phases are refined by Rietveld analysis. According to previous studies, a refined structural model showing the $P6_3/m$ symmetry and containing seven independent sites in the unit cell is used to fit the initial phase, and a refined structural model showing the $P6_3$ symmetry and containing nine independent sites in the unit cell is used to fit the high-pressure phase[28,29,37] (see Table 1). The refined structural models both significantly refine the initial (1.8 GPa) and high-pressure (15.9 GPa) phases, respectively, as shown in Figs. 4(a) and 4(b). Furthermore, the relevant Rietveld refinement parameters shown in Table 1 are reasonable,[38] confirming that the phase transition is attributed to the reduction in symmetry during the transition from the $P6_3/m$ phase to the $P6_3$ one. In addition, the refined crystal structures of the $La_{9.33}Ge_6O_{26}$ at 1.8 and 15.9 GPa are shown in the insets of Figs. 4(a) and 4(b), respectively. The SiO_4 tetrahedra displays obvious tilting, and the O3 oxygen sites split into two different 6*c* sites (O3a and O3b) during the phase transition, which could account for the reduction in symmetry during the transition from the $P6_3/m$ phase to the $P6_3$ one. The detailed structural data are listed in Table 1.

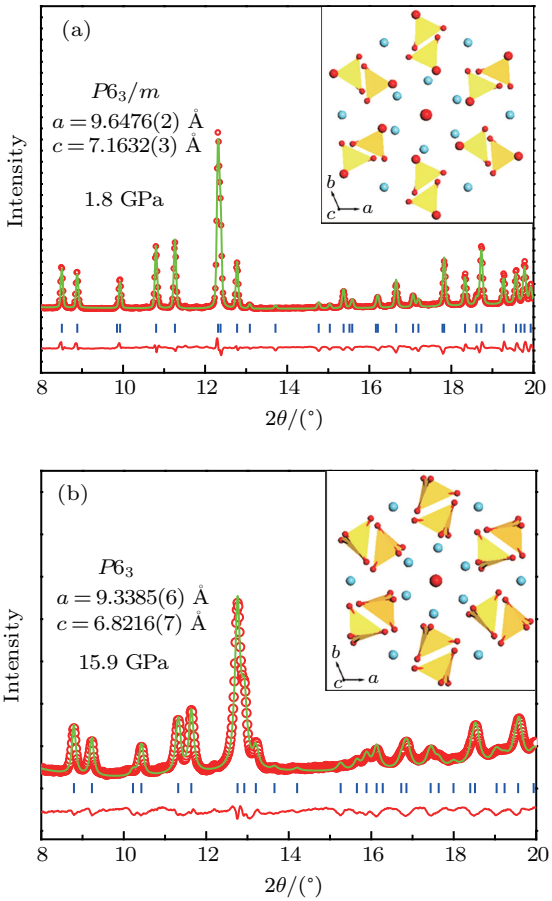


Fig. 4. (color online) Refined XRD patterns of $La_{9.33}Si_6O_{26}$ at (a) 1.8 and (b) 15.9 GPa and the corresponding refined crystal structures (the insets of (a) and (b)).

Table 1. Refined structural data of $La_{9.33}Si_6O_{26}$ at 1.8 and 15.9 GPa.

$P = 1.8$ GPa, space group: $P6_3/m$ (# 176)							$P = 15.9$ GPa, space group: $P6_3$ (# 173)					
$a = b = 9.6476(2)$ Å, $c = 7.1632(3)$ Å, $R_{wp} = 5.7\%$, $R_p = 4.2\%$							$a = b = 9.3385(6)$ Å, $c = 6.8216(7)$ Å, $R_{wp} = 6.4\%$, $R_p = 4.6\%$					
atom	site	*x*	*y*	*z*	SOF		atom	site	*x*	*y*	*z*	SOF
La1	4f	1/3	2/3	0.0185(2)	1.0		La1	2b	2/3	1/3	0.020(8)	1.0
La2	6h	0.2295(4)	–0.0163(7)	1/4	1.0		La2	2b	1/3	2/3	0.055(9)	1.0
Si	6h	0.4031(5)	0.3544(7)	1/4	1.0		La3	6c	0.214(6)	–0.017(5)	0.278 (7)	1.0
O1	6h	0.3307(5)	0.4687(9)	1/4	1.0	Si	6c	0.442(9)	0.371(6)	0.280(3)	1.0	
O2	6h	0.5832(7)	0.4924(6)	1/4	1.0	O1	6c	0.324(6)	0.491(8)	0.261(5)	1.0	
O3	12i	0.3473(9)	0.2661(8)	0.0842(5)	1.0		O2	6c	0.601(4)	0.456(7)	0.280(5)	1.0
O4	2a	0.0	0.0	1/4	1.0		O3a	6c	0.331(7)	0.291(7)	0.389(9)	1.0
							O3b	6c	0.356(7)	0.260(6)	0.030(7)	1.0
							O4	2a	0.0	0.0	0.274(6)	1.0

To further understand the structural evolution of the $La_{9.33}Si_6O_{26}$ under high pressure, *P*–*a*, *P*–*c*, *P*–*c*/*a*, and *P*–*V* are depicted in Fig. 5. The cell parameter *a* continuously varies during the phase transition (Fig. 5(a)), but the cell parameter *c* displays discontinuous variation with ∼ 1.9% *c*-axis shrinkage (Fig. 5(b)) during the phase transition, leading to a ∼ 2.2% collapse in volume (Fig. 5(d)). Furthermore, the *c*/*a* ratios of both phases gradually increase with increasing pressure

(Fig. 5(c)), indicating that the compressibility of the *a*-axis is higher than that of the *c*-axis and is related to the different arrangements of rigid SiO_4 tetrahedra along the *a*- and *c*-axes. In ATLS, the rigid SiO_4 units are directly piled along the *c*-axis, whereas there is a La–O polyhedral environment between the rigid SiO_4 tetrahedra along the *a*-axis. As a result, the *c*-axis is less compressible than the *a*-axis. In addition, compared with the axial compressible ratios of $La_{10}Si_6O_{27}$, those of $La_{9.33}Si_6O_{26}$ in both phases are slightly higher (as shown in Table 2), which could be related to the absence of interstitial oxygen atoms in the $La_{9.33}Si_6O_{26}$. According to previous studies,[29,39] compressibility is mainly dominated by the La–O polyhedral environment. In $La_{10}Si_6O_{27}$, the interstitial oxygen atoms could form larger hexahedral SiO_5 units,[35,36] compressing the La–O polyhedral environment thereby making it less compressible and further indicating that both the *a*- and *c*-axes of the $La_{10}Si_6O_{27}$ are slightly less compressive than those of the $La_{9.33}Si_6O_{26}$.

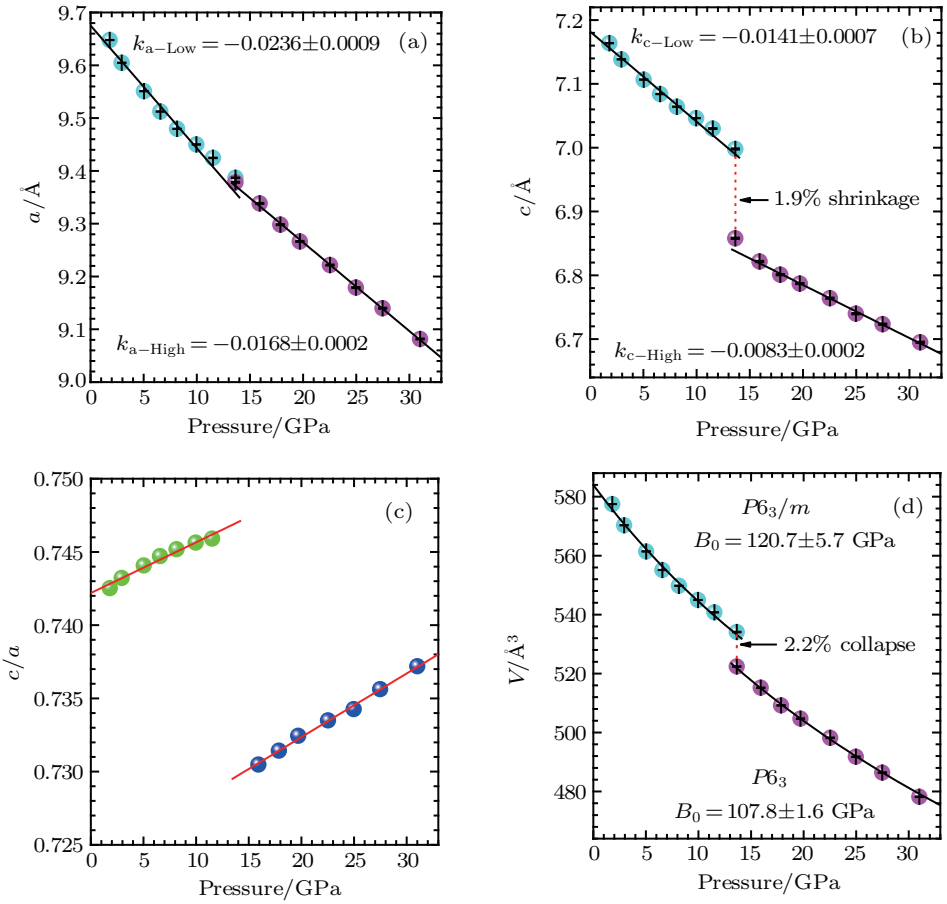


Fig. 5. (color online) Refined (a) *P*–*a*, (b) *P*–*c*, (c) *P*–*c*/*a*, and (d) *P*–*V* of $La_{9.33}Si_6O_{26}$.

Table 2. Axial compressibility ratios of $La_{9.33}Si_6O_{26}$ and $La_{10}Si_6O_{27}$ in the initial and high-pressure phases.

Composition	$k_{a-initial}$	$k_{c-initial}$	k_{a-high}	k_{c-high}
$La_{9.33}Si_6O_{26}$	–0.0236 ± 0.0009	–0.0141 ± 0.0007	–0.0168 ± 0.0002	–0.0083 ± 0.0002
$La_{10}Si_6O_{27}$	–0.0221 ± 0.0008	–0.0135 ± 0.0002	–0.0151 ± 0.0004	–0.0074 ± 0.0001

In addition, we fit the experimental pressure-volume data with the third-order Birch–Murnaghan equation of state (EOS)

$$P = 3B_0[(V/V_0)^{-7/3} - (V/V_0)^{-5/3}] \times \{1 + 3(B_0\prime - 4)[(V/V_0)^{-2/3} - 1]/4\}/2, \quad (1)$$

where V_0 is the volume per formula unit under normal pressure, V is the volume per formula unit at pressure P (in GPa), B_0 is the isothermal bulk modulus, and B_0' is the first pressure derivative of the bulk modulus. Here, B_0' = 4.74 is obtained from the F_E–f_E data of the initial phase (where $F_E = P/(3f_E(1+2f_E)^{5/2})$ is the normalized stress and $f_E = [(V_0/V)^{2/3} - 1]/2$ is the finite strain).[40,41] As shown in Fig. 5(d), the bulk modulus, B_0, of the initial phase (120.7±5.7 GPa) is unusually higher than that of high-pressure phase (107.8±1.6 GPa), implying that the high-pressure phase becomes more compressive than the initial phase and could be owing to the reduction in symmetry that occurs during the transition from the high-symmetry $P6_3/m$ phase to the low-symmetry $P6_3$ one. According to previous studies of ATLS under high pressure,[28,29] the low sym-

metry ($P6_3$) phase could afford more degrees of freedom to accommodate for the tilting of the SiO_4 tetrahedra than the high symmetry ($P6_3/m$) phase could. Moreover, the bulk moduli of both the initial (120.7±5.7GPa) and high-pressure (107.8±1.6 GPa) phases for $La_{9.33}Si_6O_{26}$ are lower than those of both the initial (128.3±1.7 GPa) and high-pressure (117.2±6.6 GPa) phases for $La_{10}Si_6O_{27}$,[29] which also could be attributed to the absence of interstitial oxygen atoms in the $La_{9.33}Si_6O_{26}$. Similar to how interstitial oxygen atoms affect the compressive behaviors of the *a*- and *c*-axes, interstitial oxygen atoms could make the La–O polyhedral environment less compressible; thus, both phases of the $La_{9.33}Si_6O_{26}$ display a lower B_0 than the $La_{10}Si_6O_{27}$.

4. Conclusions

The structural evolutions of apatite-type $La_{9.33}Si_6O_{26}$ under high pressure were systematically investigated up to 31.8 GPa, using *in situ* synchrotron XRD. A subtly reversible phase transition occurred at ∼ 13.6 GPa, which was ascribed to the reduction in symmetry during the transition from the $P6_3/m$ phase to the $P6_3$ phase, induced by the tilting of the SiO_4 tetrahedra. Furthermore, the high-pressure phase became more compressive than the initial phase, because its lower symmetry affords more degrees of freedom to accommodate for the tilting of the SiO_4 tetrahedra. Moreover, the $La_{9.33}Si_6O_{26}$ exhibited a lower P_T and a higher compressibility than the $La_{10}Si_6O_{27}$, which could be attributed to the absence of interstitial oxygen atoms in the $La_{9.33}Si_6O_{26}$. In other words, interstitial oxygen atoms could increase the P_T and lower the compressibility of the ATLS.

References

[1] Ma Y, Fenineche N, Elkedim O, Liao H and Briois P 2016 *Int. J. Hydrogen Energy* **23** 9993
[2] Dong X F, Hua G X, Dong D, Zhu W L and Wang H J 2016 *J. Power Sources* **306** 630
[3] Dai L, Han W, Li Y H and Wang L 2016 *Int. J. Hydrogen Energy* **26** 11340
[4] Kioupis D and Kakali G 2016 *Ceramics International* **8** 9640
[5] Cao X G, Jiang S P and Li Y Y 2015 *J. Power Sour.* **293** 806
[6] Xiang J, Ouyang J H and Liu Z G 2015 *J. Power Sour.* **284** 49
[7] Hori S, Takatani Y, Kadoura H, Uyama T, Fujita S and Tan T 2015 *Dalton Trans.* **44** 1755
[8] Li H, Baikie T, Pramana S S, Shin J F, Keenan P J, Slater P R, Brink F, Hester J, An T and White T J 2014 *Inorg. Chem.* **53** 4803
[9] Yin G C, Yin H, Sun M L, Zhong L H, Zhang J K, Cong R D, Gao W and Cui Q L 2014 *RSC Adv.* **4** 15968
[10] Li B Y, Liu J, Hu Y X and Huang Z X 2011 *J. Alloy. Compound.* **509** 3172
[11] Nakayama S and Sakamoto M 2013 *Solid State Ionics* **253** 47
[12] Santos M, Alves C, Oliveira F A C, Marcelo T, Mascarenhas J, Cavaleiro A and Trindade B 2013 *J. Power Sour.* **231** 146
[13] Liu W, Yamaguchi S, Tsuchiya T, Miyoshi S, Kobayashi K and Pan W 2013 *J. Power Sour.* **235** 62
[14] Fukuda K, Asaka T, Okino M, Berghout A, Béchade E, Masson O, Julien I and Thomas P 2012 *Solid State Ion.* **217** 40
[15] Orera A, Baikie T, Panchmatia P, White T J, Hanna J, Smith M E, Islam M S, Kendrick E and Slater P R 2011 *Fuel Cells* **1** 10
[16] Yoshioka H, Nojiri Y and Tanase S 2008 *Solid State Ion.* **179** 2165
[17] Baikie T, Mercier P H J, Elcombe M M, Kim J Y, Mitchell L D, White T J and Whitefield P S 2007 *Acta Crystallogr. B* **63** 251
[18] Kendrick E, Islam M S and Slater P R 2007 *J. Mater. Chem.* **17** 3104
[19] Orera A, Baikie T, Kendrick E, Shin J F, Pramana S, Smith R, White T J, Sanjuan M L and Slater P R 2011 *Dalton Trans.* **40** 3903
[20] Yoshioka H, Nojiri Y, Matsushita Y and Tanase S 2008 *Solid State Ionics* **179** 2165
[21] Ali R, Yashima M, Matsumura Y, Yoshioka H, Yoshioka H, Ohoyama K and Izumi F 2008 *Chem. Mater.* **20** 5203
[22] Yoshioka H 2007 *J. Am. Ceram. Soc.* **90** 3099
[23] Nojiri Y, Tanase S, Iwasa M, Yoshioka H, Matsumura Y and Sakai T 2010 *J. Power Sour.* **195** 4059
[24] Kendrick E, Sansom J E H, Tolchard J R, Islam M S and Slater P R 2007 *Faraday Discuss.* **134** 181
[25] Reina L L, Losilla E R, Lara M M, Bruque S, Llobet A, Sheptyakov D V and Aranda M A G 2005 *Chem. Mater.* **15** 2489
[26] Orera A, Kendrick E, Apperley D C, Orera V M and Slater P R 2008 *Dalton Trans.* 5296
[27] Tolchard J R, Islam M S and Slater P R 2003 *J. Mater. Chem.* **13** 1956
[28] Yin G C, Yin H, Wang X, Sun M L, Zhong L H, Cong R D, Zhu H Y, Gao W and Cui Q L 2014 *J. Alloy. Comp.* **611** 24
[29] Yin G C, Yin H, Zhu H Y, Wu X X, Zhong L H, Sun M L, Cong R D, Zhang J, Gao W and Cui Q L 2014 *J. Alloy. Comp.* **586** 279
[30] Hammersley A P, Svensson S O, Hanfland M, Fitch A N and H?usermann D 1996 *High Pressure Res.* **14** 235
[31] Li Q J and Liu B B 2016 *Chin. Phys. B* **25** 076107
[32] Zou Y G, Xu L, Tian K, Zhang H, Ma X H and Yao M G 2016 *Chin. Phys. B* **25** 056101
[33] Chen H Y, Xiang S K, Yan X Z, L R, Zhang Y, Liu S G and Bi Y 2016 *Chin. Phys. B* **25** 108103
[34] Errandonea D and Manjon F J 2008 *Prog. Mater. Sci.* **53** 711
[35] Matsunaga K and Toyoura K 2012 *J. Mater. Chem.* **22** 7265
[36] Kiyoshi K and Yoshio S 2014 *J. Ceram. Soc. Jpn* **122** 921
[37] White T, Ferraris C, Kim J and Madhavi S 2005 *Rev. Mineral. Geochem.* **57** 307
[38] Toby B H 2006 *Powder Diffraction* **21** 67
[39] Errandonea D, Pellicer-Porres J, Manjon F J, Segura A, Roca C F, Kumar R S, Tschauner O, Hernandez P R, Solano J L, Radescu S, Mujica A, Munoz A and Aquilanti G 2005 *Phys. Rev. B* **72** 174106
[40] Angel R J 2000 *Reviews in Mineralogy and Geochemistry* **41** 35
[41] Gomis O, Perez D S, Vilaplana R, Luna R, Sans J A, Manjon F J, Errandonea D, Gonzalez E P, Hernandez P R, Munoz A and UrsakV V 2014 *J. Alloy. Comp.* **583** 70